
Computational Geosciences **7:** 115–135, 2003.

Crossover from nonlinearity controlled to heterogeneity controlled mixing in two-phase porous media flows

Frederico Furtado [a] and Felipe Pereira [b]

[a] *Department of Mathematics, University of Wyoming, Laramie, WY 82071-3036, USA*
E-mail: furtado@uwyo.edu
[b] *Instituto Politécnico, Universidade do Estado do Rio de Janeiro, Rua Alberto Rangel, s/n, Nova Friburgo, RJ, 28601-970, Brazil*
E-mail: pereira@iprj.uerj.br

Received 26 September 2001; accepted 24 July 2002

We use high resolution Monte Carlo simulations to study the dispersive mixing in two-phase, immiscible, porous media flow that results from the interaction of the nonlinearities in the flow equations with geologic heterogeneity. Our numerical experiments show that distinct dispersive regimes occur depending on the relative strength of nonlinearity and heterogeneity. In particular, for a given degree of multiscale heterogeneity, controlled by the Hurst exponent which characterizes the underlying stochastic model for the heterogeneity, linear and nonlinear flows are essentially identical in their degree of dispersion, if the heterogeneity is strong enough. As the heterogeneity weakens, the dispersion rates cross over from those of linear heterogeneous flows to those typical of nonlinear homogeneous flows.

Keywords: fractals, heterogeneity, mixing, multiphase flow, porous media, random fields, scale up, scaling laws

1. Introduction

In this paper we investigate the complex fluid mixing in porous media flows that results from the combined effect of nonlinearities in the flow equations and geologic heterogeneities. This mixing occurs in a number of important scientific and technological contexts, including environmental remediation and the management of petroleum reservoirs. We focus on two-phase, immiscible, incompressible flow which corresponds physically to waterflooding in a petroleum reservoir. This problem is important in its own right, and also contains some of the complexities of more general reservoir displacements.

Spatial variations of naturally occurring porous formations (aquifers, petroleum reservoirs) occur at all length scales, but only the variations at the largest length scales are reliably reconstructed from the data available. The heterogeneities occurring on the smaller length scales have to be incorporated stochastically, on the basis of random

fields, in geostatistical models. As a consequence, the resulting flows through such formations are stochastic and require statistical descriptions [21].

Here we use a Monte Carlo approach for a quantitative analysis of the two-fluid mixing in heterogeneous porous media flows. This mixing is a consequence of flow velocity fluctuations about the mean flow velocity, owing to geological heterogeneities, and can be viewed as an effective dispersion process. In particular, we investigate the scaling behavior of the mixing region in the asymptotic limit of large times. As we shall see, this scaling, or growth law, is a signature of the leading mechanism governing the asymptotic dynamics of the mixing process.

The methodology employed in the present work follows closely the one developed in a series of papers (see [18, and references cited therein]) for the study of the dispersive mixing of a passive scalar by a random velocity field. We solve the fluid flow equations numerically for large ensembles of realizations of heterogeneous, nonlinear flows, and the resultant mixing region in the ensemble averaged solutions is analyzed. Specifically, we assess the relative importance of geologic heterogeneities and nonlinearities in determining fluid mixing regimes. We have conducted a parameter study varying the strength of the nonlinearity, measured in terms of the two fluids viscosity ratio, the strength of the heterogeneities and the Hurst exponent. The latter controls the nature of multiscale heterogeneity.

For the geological and fluid parameters considered here our numerical experiments suggest that the interplay between nonlinearity and heterogeneity depends on their relative strengths. In particular, mixing regions in linear and nonlinear flows grow at essentially identical asymptotic rates when heterogeneity is strong enough. As the heterogeneity weakens, the growth rates cross over to those typical of nonlinear flows in homogeneous geologies.

Our findings contribute to the discussion of the scale-up problem for flow in porous media. The level of detail incorporated into geostatistical characterizations of porous formations typically exceeds the capabilities of traditional flow simulators by a wide margin. Depending on the level of details of the geologic model, the flow process to be simulated and the computer hardware available, this disparity may be from one to several orders of magnitude. For this reason some type of coarsening or scale-up procedure is commonly used to coarsen these highly detailed geostatistical realizations to scales more appropriate for flow simulations. Such procedures aim at assigning suitable values of rock properties, mainly permeability, and other multiphase flow functions on a coarser scale suitable for computationally inexpensive fluid flow studies.

The scaling up is in general difficult. Difficulties arise both from the highly nonlinear fluid-fluid interactions in the flow of multiphase fluid mixtures and from the complex interactions between heterogeneities and nonlinearities. Most existing approaches for scaling up multiphase flow systems are based on the renormalization or "pseudoization" of the fine scale relative permeability curves to account for the effects of heterogeneities ([2,5,11] review the earlier developments; [33–35] introduce interesting, highly effective new developments). All such approaches entail a hyperbolic renormalization of the fluid transport equations in which only the first order (hyperbolic)

transport effects are modified. (Alternative scale-up methods, not based on "pseudos", are discussed in [6,9,12,23,24,26,36].) However, our results indicate that several different flow regimes occur, depending on the relative strengths of flow nonlinearity and medium heterogeneity, as well as on the spatial structure of such heterogeneity. (See also [1,17,27,32].) It is then plausible to expect that different scale-up methods (different types of coarse-scale models), tailored to the specifics of the distinct flow regimes, might provide a better coarse-grained description of the multitude of heterogeneous, multiphase flow behaviors. Thus an improved understanding of the interplay between heterogeneity and nonlinearity, as we pursue here, might provide valuable guidance for uncovering such methods and their limits.

This paper proceeds as follows. A model for the nonlinear transport problem (two-phase, immiscible flow) that we investigate appears in section 2. We describe in section 3 the model for the underlying stochastic geology used in our study. We discuss in section 4 appropriate definitions for the size of the mixing region for the case of two-phase, nonlinear flows. In section 5 the mixing processes in two limiting situations, nonlinear homogeneous and linear heterogeneous transport problems, are considered and some new numerical results for the linear problem are presented. Our main results appear in section 6. The relative importance of nonlinearity and heterogeneity is carefully investigated for the nonlinear transport problem considered here. Further discussion and conclusions appear in section 7.

2. Governing equations

We study two-phase flow in the viscous-dominated flow limit. Thus we neglect the effects of gravity, compressibility and capillarity and set the porosity equal to a constant. The two phases will be referred to as water and oil, and indicated by the subscripts w and o, respectively. Darcy's law for each phase then takes the form:

$$\mathbf{u}_i = -\frac{k_{\mathrm{r}i}(s)}{\mu_i} k(\mathbf{x}) \nabla p,$$

where $\mathbf{u}_i$ is the phase velocity, k is the absolute permeability, $k_{\mathrm{r}i}$ is the relative permeability and μ_i is the viscosity, each with respect to phase i, s is the water saturation, and p is the pressure. Darcy's law combined with the conservation laws for the phases can be expressed in the familiar form of "pressure" and "saturation" equations:

$$\mathbf{u} = -\lambda(s) k \nabla p, \qquad \nabla \cdot \mathbf{u} = 0, \tag{1}$$

$$\frac{\partial s}{\partial t} + \nabla \cdot \big(f(s) \mathbf{u} \big) = 0. \tag{2}$$

(The constant porosity has been scaled out by a change of the time variable.) Here, λ is the total mobility, f is the fractional flow of water, and $\mathbf{u}$ is the total velocity. These parameters are given as

$$\lambda(s) = \frac{k_{\mathrm{rw}}(s)}{\mu_{\mathrm{w}}} + \frac{k_{\mathrm{ro}}(s)}{\mu_{\mathrm{o}}}, \qquad f(s) = \frac{k_{\mathrm{rw}}(s)/\mu_{\mathrm{w}}}{\lambda(s)}, \qquad \mathbf{u} = \mathbf{u}_{\mathrm{w}} + \mathbf{u}_{\mathrm{o}}.$$

The relative permeabilities are assumed to be quadratic in form:

$$k_{\mathrm{ro}}(s) = \left(1 - (1 - s_{\mathrm{ro}})^{-1} s\right)^2, \qquad k_{\mathrm{rw}}(s) = (1 - s_{\mathrm{rw}})^{-2}(s - s_{\mathrm{rw}})^2,$$

where s_{ro} is the residual oil saturation and s_{rw} is the connate water saturation. This choice corresponds to immiscible flow.

We consider equations (1), (2) in a two-dimensional rectangular domain $\Omega = (0, L_x) \times (0, L_y)$, with the boundary conditions

$$\begin{aligned} \mathbf{u} \cdot \mathbf{n} &= -q, \quad && \text{on } x = 0, \\ p &= 0, && \text{on } x = L_x, \\ \mathbf{u} \cdot \mathbf{n} &= 0, && \text{on } y = 0, L_y, \end{aligned} \tag{3}$$

where $\mathbf{n}$ is the outward-pointing normal vector to $\partial\Omega$, and a uniform initial condition

$$s(\mathbf{x}, 0) = s_0. \tag{4}$$

The boundary conditions (3) simulate a left-to-right waterflood. Water is injected uniformly (at a constant rate q) through the left vertical boundary ($x = 0$) of Ω, no flow conditions are imposed along the horizontal boundaries ($y = 0, L_y$), and fluid is produced from a well kept at constant (zero) pressure at the right vertical boundary ($x = L_x$).

We solve equations (1), (2) using a standard IMPES (implicit in pressure, explicit in saturation) method. This method combines a hybridized mixed finite element method [10], which is equivalent to cell-centered finite differences, for the solution of the pressure equation with a second order, non-oscillatory central finite difference scheme [28] for the solution of the saturation equation. The resulting overall numerical scheme is effective in treating the rapidly changing permeabilities that arise from stochastic geology, produces accurate velocity fields and resolves the sharp saturation fronts with small numerical diffusion [38]. Details of our implementation of this numerical scheme will appear elsewhere [16].

3. Description of permeability fields

In this paper we consider scalar, log-normal permeability fields,

$$k(\mathbf{x}) = k_0 \mathrm{e}^{\rho \xi(\mathbf{x})}, \tag{5}$$

where ξ is a stationary Gaussian random field, characterized by its mean $\langle \xi \rangle = 0$ (angle brackets denote ensemble averaging) and its covariance function

$$C(\mathbf{x}, \mathbf{y}) = \left\langle \xi(\mathbf{x}) \xi(\mathbf{y}) \right\rangle.$$

The mean $\langle k \rangle$ and variance σ_k^2 of the log-normal field k are set by the coefficients k_0 and ρ. Changing ρ varies the coefficient of variation,

$$CV_k \equiv \frac{\sigma_k}{\langle k \rangle}, \tag{6}$$

of the permeability field. We use the coefficient of variation as a dimensionless measure of the heterogeneity of the permeability field. We take the field ξ to be isotropic and, to introduce variability over all length scales, fractal, or self-similar. Thus its covariance function is given by a power law:

$$C(\mathbf{x}, \mathbf{y}) = |\mathbf{x} - \mathbf{y}|^{\beta}, \quad \beta < 0. \tag{7}$$

The scaling exponent β, known as the Hurst exponent, controls the degree of multiscale heterogeneity: as it increases, the heterogeneities concentrated in the larger length scales are emphasized and the field becomes more regular (locally).

The fractal statistics (7) is singular at short distances; however its realization on a finite lattice provides a short distance regularization due to the lattice cutoff. See [1,18] for a discussion of the use of fractal random fields as a model of geological variability in studies of fluid flow through natural porous media; see [13,14] for the numerical construction of fractal Gaussian random fields.

4. Scaling analysis of mixing dynamics

A quantitative analysis of the mixing process is afforded by analysis of the growth rate of the mixing region as a function of time or, equivalently, travel distance. For this purpose, we introduce a time dependent length scale, which we dub the mixing length, characteristic of the (longitudinal) extent of the mixing region and study its growth as a function of time or travel distance. The mixing region scaling exponent is the slope in a log–log plot of the mixing length vs. time or travel distance. A scaling exponent equal to 0.5 corresponds to the large time asymptotic behavior of classical (Fickian) diffusion. A scaling exponent equal to 1.0 corresponds to a "convective" mixing regime, characteristic of viscous fingering driven by the nonlinear instability of the flow (see section 5.1 below).

In section 4.1 we study the mixing process for an idealized model problem. In section 4.2 the results are used to motivate our definition of mixing length.

4.1. A model problem

Consider the one-dimensional convection–diffusion problem:

$$\frac{\partial c}{\partial t} + u\frac{\partial c}{\partial x} - \nu(t)\frac{\partial^2 c}{\partial x^2} = 0, \tag{8}$$

$$c(x, 0) = \begin{cases} c_- & \text{when } x < 0, \\ c_+ & \text{when } x > 0. \end{cases} \tag{9}$$

Equation (8) is a simplified form of the effective equation for the dispersive mixing of a passive scalar by a random velocity field obtained via perturbation theory [18,37]. Here c is the concentration of the scalar, and the constants c_- and c_+ define the initial concentration. As it is our intention to use the model problem (8), (9) to develop a methodology applicable for the analysis of the waterflooding problem, we take $c_- > c_+$.

The solution c_ν of equations (8), (9) is given by the complementary error function:

$$c_\nu(x,t) = \frac{(c_- - c_+)}{2}\operatorname{erfc}\left(\frac{x-ut}{\ell(t)}\right) + c_+, \tag{10}$$

where

$$\ell(t) \equiv 2\left[\int_0^t \nu(\sigma)\,\mathrm{d}\sigma\right]^{1/2}.$$

The similarity solution (10) defines two characteristic length scales of the mixing process: $L(t) \equiv ut$ and $\ell(t)$. The former represents the (mean) distance traveled by the mixing layer over the time period t; the latter furnishes a measure of the length of the mixing layer at time t. In the following, we explain how to obtain the length scale $\ell(t)$ without explicit reference to the solution (10), in a manner which can be carried over to the nonlinear flow problems that we study. This will allow us to introduce a proper definition of "mixing length" in those cases.

If we drop the diffusive flux $(-\nu(t)\partial c/\partial x)$ from the transport problem (8), (9), its solution is given by the Heaviside function:

$$c_0(x,t) = (c_- - c_+)H\big(L(t) - x\big) + c_+; \tag{11}$$

i.e., the initial interface at $x = 0$ separating the two fluids is simply moved to the new location $x = L(t)$ at time t. The difference in the spatial distribution of "mass" in the solutions (10) and (11),

$$\mathcal{M}(t) \equiv \int_{-\infty}^{\infty} \big|c_\nu(x,t) - c_0(x,t)\big|\,\mathrm{d}x,$$

is the effect of diffusion (present in the former but not in the latter), which transports "mass" from the region $x < L(t)$ to the region $x > L(t)$. Thus,

$$\frac{1}{2}\mathcal{M}(t) = \int_{-\infty}^{L(t)} \big|c_\nu(x,t) - c_0(x,t)\big|\,\mathrm{d}x \tag{12}$$

$$= \int_0^t -\nu(\sigma)\frac{\partial c_\nu}{\partial x}\big(L(\sigma),\sigma\big)\,\mathrm{d}\sigma = \frac{(c_- - c_+)}{\sqrt{\pi}}\int_0^t \frac{\nu(\sigma)}{\ell(\sigma)}\,\mathrm{d}\sigma. \tag{13}$$

Next, if we substitute the identity

$$\frac{1}{2}\frac{\mathrm{d}\ell(t)}{\mathrm{d}t} = \frac{\nu(t)}{\ell(t)}$$

into equation (13) and notice that $\ell(0) = 0$, we obtain $\ell(t)$ from $\mathcal{M}(t)$:

$$\ell(t) = \frac{\sqrt{\pi}}{c_- - c_+}\mathcal{M}(t). \tag{14}$$

4.2. The mixing length

Our choice of boundary conditions (cf. section 2), in particular the specification of a constant injection rate to drive the bulk incompressible flow, forces the total flow rate $\bar{u}_x$ in each realization of the porous system to be the same constant:

$$\bar{u}_x \equiv \int_0^{L_y} u_x(x, y, t)\, \mathrm{d}y = qL_y.$$

(u_x is the component of the flow velocity $\mathbf{u}$ in the horizontal direction x; L_y is the length of the porous system in the vertical direction y.) As a consequence, the fluctuations in the flow velocity $\mathbf{u}$ around the mean $\langle \mathbf{u} \rangle = (q, 0)$, owing to stochastic and nonlinear effects, result in the spreading of the heterogeneous saturation fronts around the location of the planar front in the saturation solution of equations (1)–(4) with a constant permeability (homogeneous geology). See figure 1. The effect of this spreading is diffusive in the sense that the transversely averaged saturation around the latter location is spread out. This situation is analogous to the diffusion observed in the solution c_v of our model problem (8), (9) around the location $L(t)$ of the sharp interface in c_0. Thus we can use equation (14) to motivate the definition of mixing length in our study of two-phase flow in heterogeneous systems.

Given that we employ Monte Carlo simulations (in the general sense) in this study, we are confronted with two possibilities to define the mixing length. One possibility is to define it for each realization, or sample, in the ensemble of stochastically-generated permeability fields $k(\mathbf{x})$. In this approach, for each realization of the permeability field we solve numerically equations (1)–(4) and the computed saturation s is then averaged in the direction transverse to the mean flow (the y-direction) to define $\bar{s} = \bar{s}(x, t)$. Note that $\bar{s}$ is defined by a spatial average, and is thus a random variable. Next, S_H, the saturation solution of equations (1)–(4) with a constant permeability, e.g., $\bar{k} \equiv \langle k(\mathbf{x}) \rangle$, is computed and used to define the mixing length for that particular realization:

$$\ell_{\mathrm{r}}(t) \equiv \frac{1}{(s_- - s_+)} \int_0^{L_x} \left| \bar{s}(x, t) - S_H(x, t) \right| \mathrm{d}x. \tag{15}$$

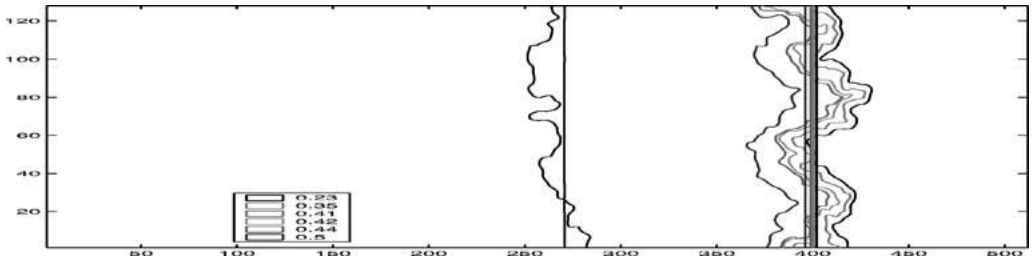

Figure 1. Saturation profile for two-phase flow with viscosity ratio $M = \mu_{\mathrm{o}}/\mu_{\mathrm{w}} = 5$ in a $\beta = -\infty$ permeability field (ragged contours). Superposed is the planar saturation profile for the corresponding homogeneous flow.

Here, L_x is the length of the computational domain in the horizontal direction x, and s_- (respectively s_+) is the saturation value immediately behind (respectively ahead) the saturation front in the solution S_H. In our case, s_+ will always be the (constant) initial saturation s_0 (see equation (4)). The value of s_- depends on the viscosity ratio $M = \mu_o/\mu_w$, through the dependence of the fractional flow function f on M, and s_+; its determination is a simple exercise in the theory of hyperbolic conservation laws (see, e.g., [31]). We note in passing that the solution S_H is independent of the choice of the constant permeability value.

In the stochastic context, ℓ_r is a random variable, and should be specified in terms of its statistical moments. In particular, the expected value

$$\ell_m(t) \equiv \left\langle \ell_r(t) \right\rangle$$

is the best estimate of the spreading, or dispersion, of each sample $\bar{s}$ around the planar front of the homogeneous profile S_H. In other words, ℓ_m gives the best estimate of the size of the mixing region in each sample solution s, and should be adopted as the definition of mixing length.

An alternative possibility is to base the definition of mixing length on the dispersion of the ensemble. In this approach, the samples $\bar{s}$ are averaged across the ensemble, and the resulting profile $\bar{s}_e(x,t) \equiv \langle \bar{s}(x,t) \rangle$, which is an estimate for the mean saturation $\langle s \rangle$, is used to define the ensemble based mixing length:

$$\ell_e(t) \equiv \frac{1}{(s_- - s_+)} \int_0^{L_x} \left| \bar{s}_e(x,t) - S_H(x,t) \right| \mathrm{d}x. \tag{16}$$

ℓ_e estimates the dispersion of the mean saturation $\langle s \rangle$ around the front of the homogeneous solution S_H.

The distinction between dispersion based on the ensemble and dispersion based on single realizations is discussed in [1,7,8,29] in the case of linear flow (tracer and solute

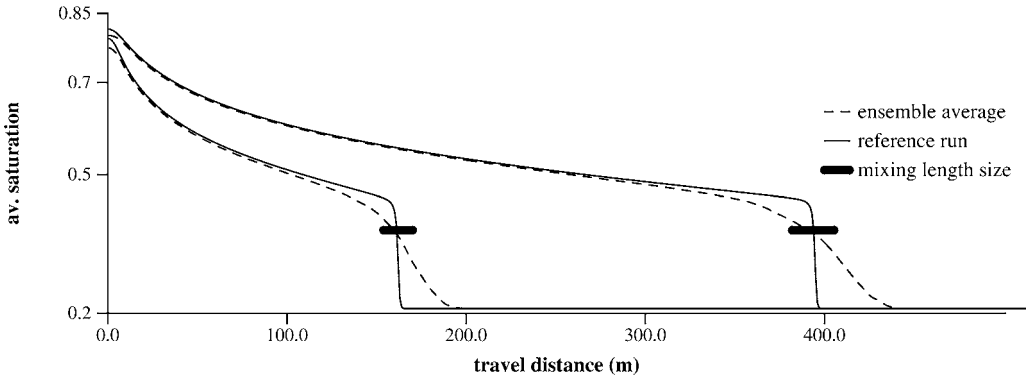

Figure 2. $\bar{s}_e$ profiles (dashed curves) for $M = 5$ flow in an ensemble of $\beta = -\infty$ permeability fields at representative times. Superposed upon them are the S_H profiles (solid curves) of the corresponding homogeneous run at the same times. Also shown (dark solid lines) is the actual size of the computed mixing length ($\sqrt{\pi}\ell_e$).

transport). We examine this question in the context of our methodology in section 6.2, and our main conclusion is stated here. In brief, the mixing lengths computed using each of the two viewpoints are indistinguishable in our case. Consequently, hereafter we will adopt ℓ_e as our definition of mixing length, and will only discuss the results obtained via this definition.

Figure 2 illustrates the homogeneous profile S_H and the ensemble averaged saturation profile $\bar{s}_e$ used in the computation of the mixing length for a $\beta = -\infty$ permeability field. Also shown in this figure is the mixing length $\ell_e(t)$ for two times.

5. Mixing regimes: single effect cases

Both nonlinearity of the flow equations and permeability heterogeneity can cause dispersive mixing of the fluid transport in porous media. In certain parameter regimes, the nonlinear coupling of the saturation equation to Darcy's law causes the unstable growth of small fluctuations in saturation fronts into a highly-fingered flow pattern (viscous fingering; see, e.g., [22]). Heterogeneities in permeability cause velocity variations which in turn introduce dispersion into the fluid flux and the development of highly conductive flux channels. The two mechanisms, nonlinearity and heterogeneity, interact since heterogeneity can trigger fingers and influence their subsequent dynamics. To understand the combined effect of heterogeneity and nonlinearity on the mixing process, it is convenient first to consider each effect separately.

5.1. The effect of nonlinearity

For *nonlinear* flow in *homogeneous* porous media, a linear stability analysis (infinitesimal perturbations of the displacement front and short periods of time) is instructive in identifying important parameters and regimes. When applied to equations (1), (2), this analysis reveals the existence of two distinct flow regimes, characterized in terms of a dimensionless parameter Λ, the frontal mobility ratio [3,4,30],

$$\Lambda = \frac{\lambda(s_-)}{\lambda(s_+)}, \quad 0 < \Lambda < 2; \tag{17}$$

s_+, s_- are the saturation values ahead and behind the saturation front, respectively. In the region $0 < \Lambda < 1$ the flow is stable, and small amplitude perturbations in the saturation fronts decay, whereas in the region $1 < \Lambda < 2$ the flow is unstable, and such perturbations grow. (See also [20] for a stability analysis of finite amplitude perturbations leading to the same conclusions.) If the effects of capillarity are considered, capillary forces mitigate the instability, but only to a limited extent [25]. Basically, they introduce a cutoff on the wavelength of fluctuations that grow unstably.

For our choice of relative permeability functions, the critical value $\Lambda = 1$ separating the stable and unstable regimes corresponds to a viscosity ratio $M = \mu_o/\mu_w = 2.657$, with values of $M > 2.657$ (respectively $M < 2.657$) in the unstable (respectively stable) regime.

Linearized stability analyses provide information on the inception of instability for small amplitude perturbations, but give no information on the large time nonlinear development of perturbations after a loss of stability. We have investigated such dynamics via direct numerical simulations of the nonlinear flow equations. It is expected that a variety of factors can affect this dynamics. These include mobility ratio of the fluids present, strength of capillary forces and injection rate of displacing fluid. Under the same flow conditions of the present study (i.e., same boundary conditions, flow domain aspect ratio and local multiphase flow functions) our results in [15] indicate that, to a first approximation, the size of the mixing region (as defined in section 4.2) in an unstable flow process grows linearly with time, for large time:

$$\ell_e(t) = \mathrm{O}(t), \quad \text{as } t \to \infty. \tag{18}$$

We shall hereafter refer to a flow regime wherein the mixing length obeys the scaling law (18) as *nonlinear unstable* (NU). Similarly, we shall refer to a stable flow process wherein the long time behavior of the mixing region is

$$\ell_e(t) = \mathrm{O}(1), \quad \text{as } t \to \infty, \tag{19}$$

as *nonlinear stable* (NS).

5.2. The effect of heterogeneity

Linear transport (e.g., tracer flow) in *heterogeneous* porous media is described by the following transport equation for the scalar field $s(\mathbf{x}, t)$ (tracer concentration):

$$\frac{\partial s}{\partial t} + \mathbf{u} \cdot \nabla s = \nu \Delta s, \tag{20}$$

where ν is the (constant) molecular diffusivity and the random velocity field $\mathbf{u}$ is given by Darcy's law and the condition of incompressibility (cf. equations (1), (2))

$$\mathbf{u} = -\frac{k(\mathbf{x})}{\mu} \nabla p, \quad \nabla \cdot \mathbf{u} = 0. \tag{21}$$

(In tracer flows, the two fluids are miscible and have equal viscosities μ. In this case, the local flow of each fluid is proportional to its concentration (i.e., the relative permeabilities are s and $1 - s$ for the tagged and untagged fluids, respectively), and the total mobility $\lambda(s) \equiv 1/\mu$.)

Assuming the log-permeability $\xi(\mathbf{x}) = \ln k(\mathbf{x})$ to be a Gaussian random field with a power law covariance of the form (7), the theory developed in [18] (see also the references cited therein) provides the following scaling laws for the asymptotic behavior of the mixing length $\ell(t)$, defined in terms of the complementary error function solution of the effective equation satisfied by the average field $\langle s \rangle$ (see equation (10)):

$$\ell(t) = \mathrm{O}\big(t^{\gamma}\big), \quad \text{with } \gamma = \max\left\{\frac{1}{2}, \frac{1}{2} + \frac{1+\beta}{2}\right\}. \tag{22}$$

Two distinct qualitative regimes can be seen by examining (22). If $\beta \leqslant -1$, then $\gamma = 1/2$, and the mixing process is Fickian. If $-1 < \beta < 0$, then $\gamma > 1/2$, and the mixing is anomalous, or scale dependent (i.e., the diffusivity increases with time or, equivalently, with travel distance).

We notice that for linear flow the frontal mobility ratio $\Lambda \equiv 1$ and the flow is neutrally stable with respect to viscous fingering. Therefore the mixing (22) is solely the effect of velocity dispersion caused by (permeability) heterogeneity. We shall hereafter refer to a mixing regime having the scaling behavior (22) as *linear* (L).

The scaling relations (22) were derived by a second order perturbation theory applied to the fluid transport equation (20). As such, they are only expected to be valid under the assumption of weak velocity fluctuations, the perturbation parameter. However, direct numerical integration [18] of the flow problem (20), (21) confirms these scaling relations even for velocity fields produced from permeability fields with large heterogeneity strength.

As part of the present study, we have verified the validity of the scaling relations (22) in a regime where perturbation theory should not be applicable, due to the strength of the velocity fluctuations. Table 1 lists the coefficients of variation for the permeability fields CV_k and the corresponding velocity fields CV_u, used in this study. Each CV value in table 1 (and also in tables 3 and 4 below) is the average value over the ensemble of realizations of permeability fields, or the corresponding velocity fields,

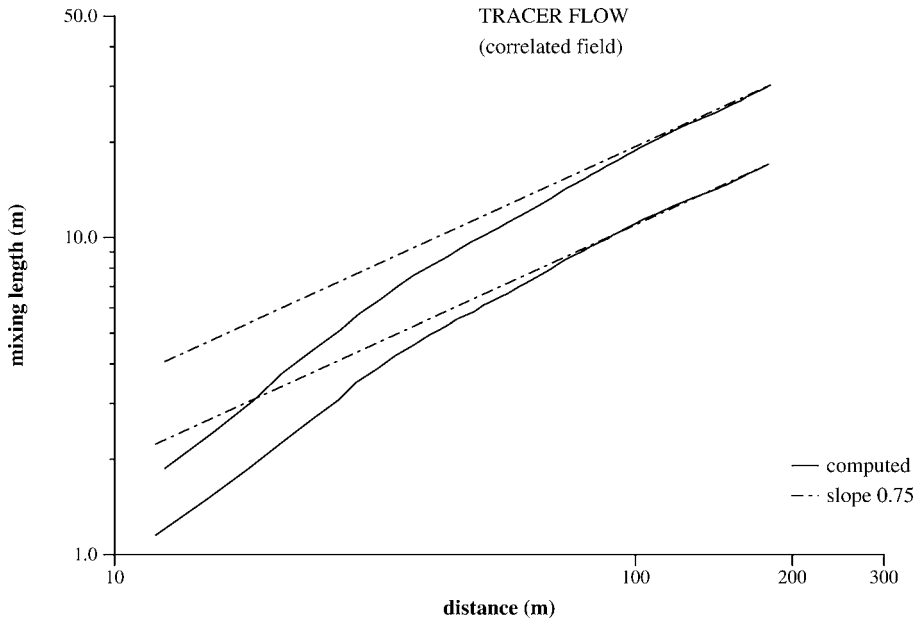

Figure 3. Log–log plot of mixing length as a function of travel distance for tracer flow subject to strong heterogeneities. The solid lines are the computed mixing lengths. The dashed straight lines are plotted for comparison, and have slope 0.75, the growth rate predicted by perturbation theory for $\beta = -0.5$. The CV_k values are 8.4 (top) and 2.6 (bottom).

Table 1
Velocity field CV_u for tracer flow simulations as a function of permeability field CV_k for the two values of β considered.

CV_k/β	$-\infty$	-0.5
2.6	0.5	0.9
3.5	0.9	
8.4		1.4

used in the simulations. We remark that the largest values for CV_u are close to (or even larger than) one, thus beyond the limit adequate for a perturbation theory. However, we observed good agreement between the simulation results and the theoretical prediction (22) over the full range of CV values in table 1. See figure 3 where we display the results for $\beta = -0.5$. The curves in this figure, which we term "mixing length curves", plot the mixing length as a function of travel distance, in log–log scale.

It is emphasized that in our simulations of two-phase flow (see section 6) the values of CV_k used for each value of β considered are all smaller than the corresponding largest ones in table 1. Thus for these simulations the dispersive mixing that would result from heterogeneity alone (i.e., in a tracer flow) would satisfy the scaling laws (22).

6. Mixing regimes: combined effect cases

6.1. Description of Monte Carlo simulations

All results in this paper are for a flow region which is four times longer in the mean flow direction (the horizontal direction x) than in the transverse direction (the vertical direction y): $L_x/L_y = 4$. All log-permeability fields were drawn from a Gaussian distribution with the power law covariance described in section 3. Two permeability exponents, $\beta = -\infty, -0.5$, and several values for the permeability coefficient of variation, CV_k, were considered. The rationale for this choice of exponents is the desire to explore the effect of short length ($\beta = -\infty$) and long length scale ($\beta = -0.5$) (permeability) heterogeneities in two-phase flow dispersion. In the case of linear flow, these exponents lead to Fickian and anomalous dispersion, respectively. See section 5.2.

The computations involved the construction of the various ensembles of random permeability fields, characterized by different values of the exponent β and the coefficient of variation CV_k, and the subsequent determination of the resultant mixing region for the fluid flows through these ensembles. Both numerical and statistical convergence were verified by successive mesh refinements and increase in ensemble size, respectively. For each of the final flow studies, an ensemble of 14 distinct permeability realizations was used. Table 2 lists the grid sizes for the final computations of the fluid flows (computational grid) and for the specification of the absolute permeability (heterogeneity grid). The flow grids used resolve the fine details of the velocity fluctuations induced by the heterogeneities in the permeability grid.

Table 2
Grid sizes.

β	$-\infty$	-0.5
Computational grid	512×128	512×128
Heterogeneity grid	256×64	512×128

The initial water saturation s_0, the residual oil saturation s_{ro}, and the connate water saturation s_{rw} were set equal to the following values: $s_0 = 0.21$, $s_{\mathrm{ro}} = 0.15$, $s_{\mathrm{rw}} = 0.2$. We do not expect these parameters to affect the nature of the results of our study, whose focus is on the role of nonlinearity and heterogeneity in determining fluid mixing regimes.

6.2. Ensemble based vs. realization based mixing length

Here we examine the two possible definitions of mixing length, ℓ_e and ℓ_m (cf. section 4.2). The situation displayed in figure 4 represents the typical case encountered in our study. In this figure we consider flow problems with the following selection of parameters: $\beta = -0.5$, $CV_k = 1.83$, $M = 2.657$ (top picture) and $\beta = -\infty$, $CV_k = 2.93$, $M = 5.0$ (bottom picture). Three types of curves are presented, each giving a mixing length as a function of travel distance. The various dotted lines are the mixing lengths of various single realizations. Each dotted line represents a random variable ℓ_{r}, the single realization mixing length for the given realization of the permeability field. The expected value of the single realization mixing length ℓ_m is shown in the dashed line. Finally, the solid line is the mixing length of the ensemble, ℓ_e. The coincidence of ℓ_m and ℓ_e is evident.

It can be inferred from the discussions in [1,7,8,29] that the difference between ensemble based and single realization based mixing lengths, when it exists, is due to the uncertainty, or randomness, in the single realization mean position $L_{\mathrm{r}} = L_{\mathrm{r}}(t)$ of the mixing region. Note that L_{r} is defined by transverse averages, not ensemble averages, and is in principle a random variable. The effect of this uncertainty is dispersive and an estimate of its extent is given by the variance $\langle (L_{\mathrm{r}} - \langle L_{\mathrm{r}} \rangle)^2 \rangle^{1/2}$.

In our study L_{r} is no longer a random variable. Indeed, it is given by the location of the saturation shock in the homogeneous solution S_H. This is a consequence of our choice of boundary conditions (constant injection rate) and the incompressibility of the flow. Thus the mechanism responsible for the difference between ensemble based and realization based mixing lengths is suppressed, and both definitions agree in our case.

6.3. Mixing regimes for heterogeneous, two-phase flow

Tables 3 and 4 summarize our results for $\beta = -\infty$ and $\beta = -0.5$, respectively. These tables display the values of the viscosity ratio M and coefficient of variation CV_k, used in each study, and the corresponding large time asymptotic mixing regimes. The

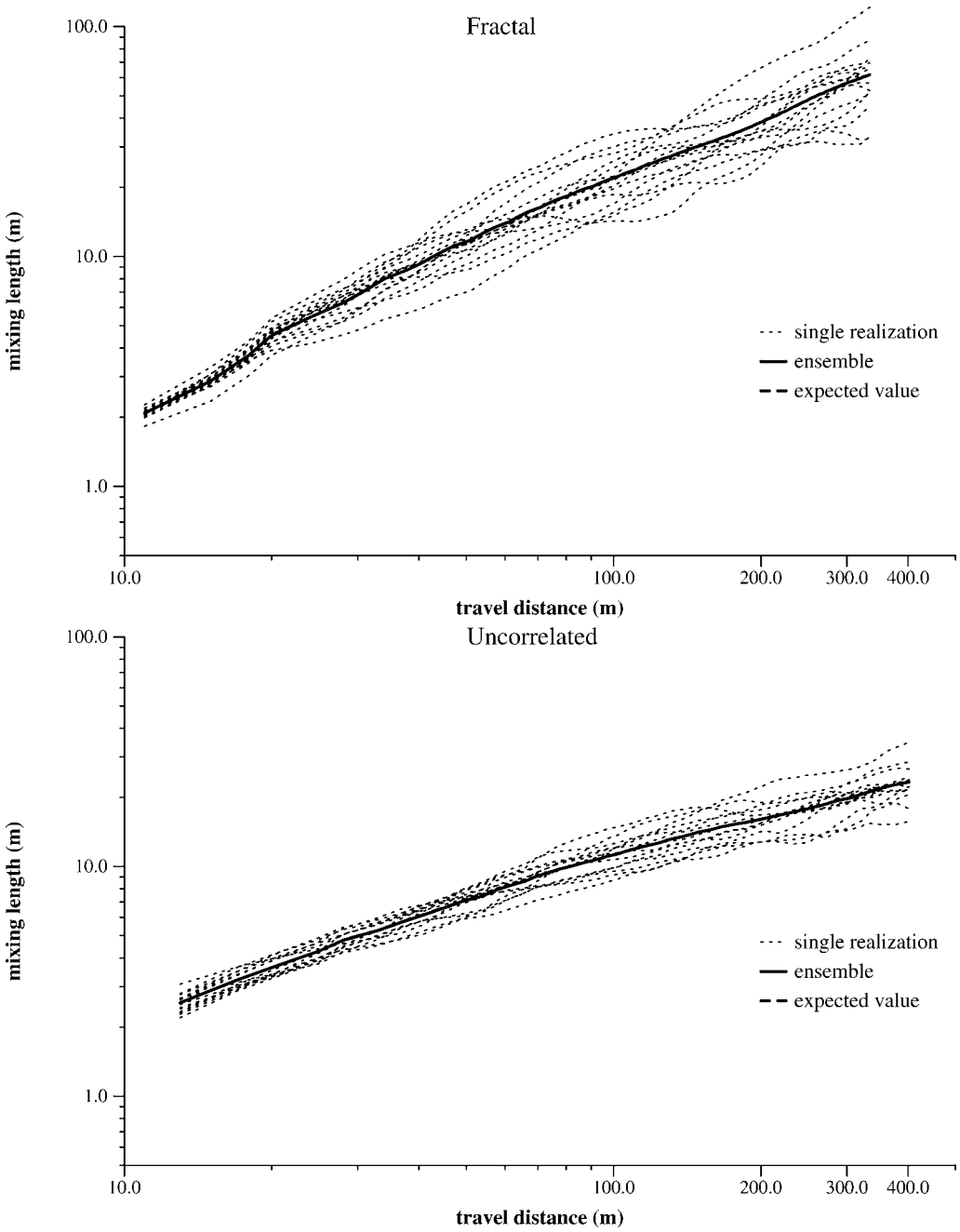

Figure 4. Comparison of the ensemble of individual realization mixing lengths (various dotted curves), the mean of the individual realization mixing lengths (dashed curve), and the ensemble mixing length (solid curve). For the top (respectively bottom) picture $M = 2.657$ (respectively $M = 5$), $\beta = -0.5$ (respectively $\beta = -\infty$), and $CV_k = 1.83$ (respectively $CV_k = 2.93$). The expected value and ensemble mixing length curves coincide.

Table 3
$\beta = -\infty$.

M/CV_k	0.54	1.33	2.93
20	NU	NU	NU
10	NU	NU	L^+
5	NU	L^+	L
2.657	L	L	L
1	L^-	L^-	L^-
0.5	NS		

Table 4
$\beta = -0.5$.

M/CV_k	0.49	0.99	1.83
20	NU	NU	NU
5	NU	NU	L
2.657	L^+	L	L
1	L^-	L^-	L^-
0.5	L^-		

mixing regimes are classified according to the growth of $\ell_e(t)$ in terms of an asymptotic scaling law, $\ell_e(t) = O(t^\delta)$, as $t \to \infty$, as follows:

- NU (Nonlinear Unstable) if $\delta = 1$ (see section 5.1);
- NS (Nonlinear Stable) if $\delta = 0$ (see section 5.1);
- L (Linear) if $\delta = \gamma$;
- L^+ (Superlinear) if $\gamma < \delta < 1$;
- L^- (Sublinear) if $0 < \delta < \gamma$.

γ is the scaling exponent for the linear flow problem; it depends on β and is given in (22) (see section 5.2).

6.4. Discussion

We focus the discussion on the relative importance of nonlinearity and heterogeneity in the fluid mixing dynamics.

Consider the case $\beta = -\infty$ first. Figure 5 corresponds to the results in the fourth row of table 3. These results pertain to a study in which the nonlinearity strength is kept fixed, by fixing $M = 5$, whereas the heterogeneity strength is varied. Each picture in this figure shows the log–log plot of the mixing length ℓ_e as a function of the travel distance (the irregular curve). Also plotted are two straight lines with vertical positions fixed to agree with the last plotted point on the mixing length curves. The slopes of these lines are 0.5, the scaling exponent of the linear mixing regime L for this value of β, and 1, the scaling exponent of the nonlinear unstable mixing regime NU. It is clear

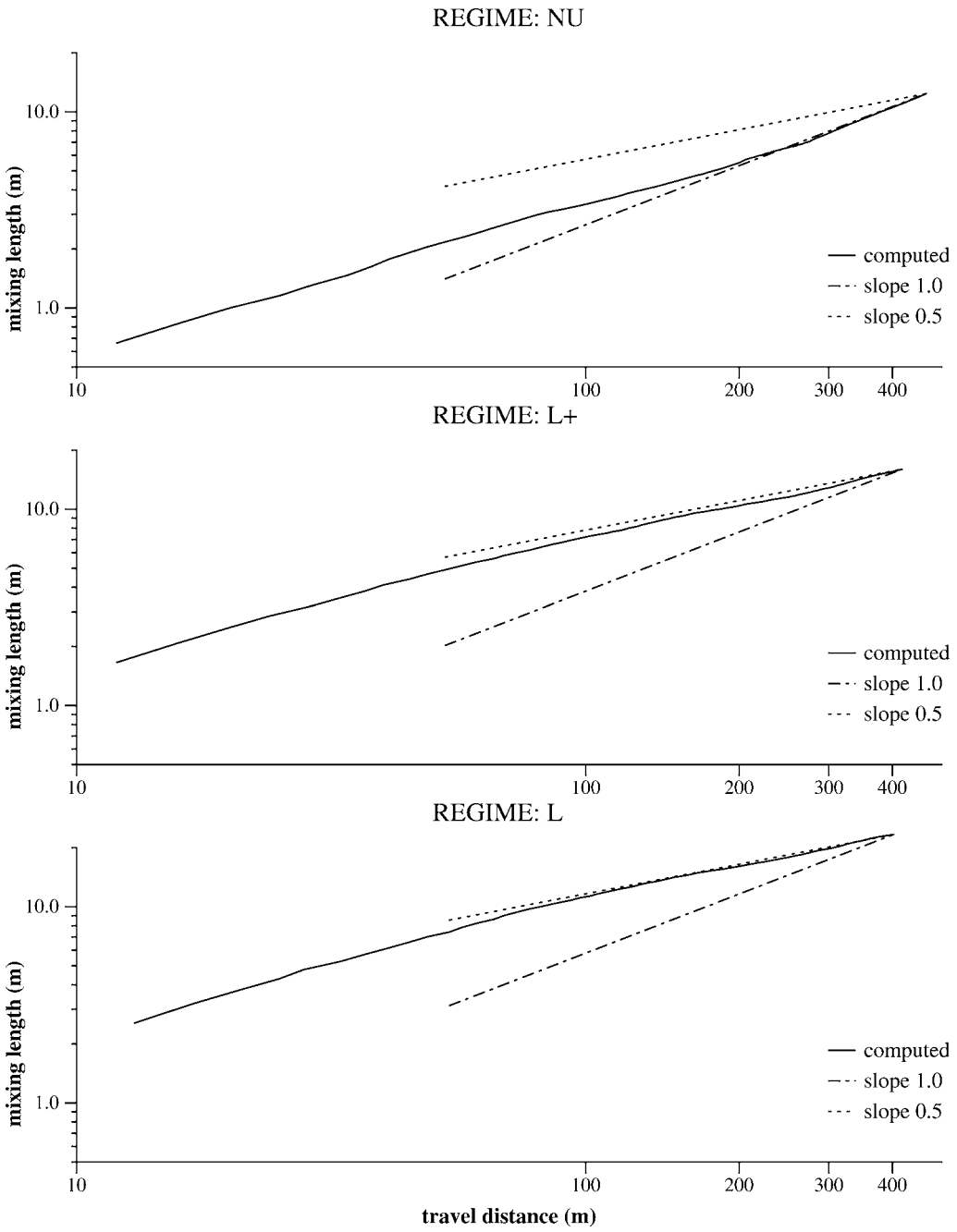

Figure 5. Log–log plot of mixing length as a function of travel distance for two-phase flow ($M = 5.0$) in $\beta = -\infty$ permeability fields corresponding to distinct mixing regimes. From top to bottom the CV_k values are: 0.54, 1.33 and 2.93; cf. fourth row of table 3.

that as the value of CV_k is increased the mixing length curves bend continuously from the NU regime towards the L regime.

The results in the third column of table 3 pertain to a study in which the heterogeneity strength is kept fixed, by fixing $CV_k = 1.33$, and the nonlinearity strength M is varied. As M is decreased, several distinct mixing regimes occur, ranging from the nonlinear unstable regime NU to the sublinear regime L^-.

The results for $\beta = -0.5$ show the same overall behavior as the ones for $\beta = -\infty$. As the relative strengths of nonlinearity and heterogeneity are varied, distinct mixing regimes are observed, ranging from the linear regime L, when the heterogeneity dominates, to the nonlinear regimes NU and NS, when the nonlinearity dominates. Figure 6 shows saturation surface plots used in the ensemble averages which led to the results reported in the third column of table 4. The displacements pictured in figure 6 all use the same realization of permeability field characterized by $\beta = -0.5$ and $CV_k = 0.99$. From top to bottom, three values for M were considered: 1.0, 2.657 and 5.0. The surface plots in this figure are displayed at different times corresponding to the same travel distance of the corresponding mixing regions.

Our findings can be summarized as follows:

- Distinct mixing regimes, characterized by the asymptotic scaling behavior of the mixing region, occur depending on whether one of the driving mechanisms (nonlinearity and heterogeneity) dominates the mixing dynamics or not.
- If nonlinearity dominates, then two distinct mixing regimes are possible, according to whether the nonlinear effects are stabilizing (NS regime) or destabilizing (NU regime).
- If heterogeneity dominates, then the linear regime L is observed. In this case, mixing regions in linear and nonlinear flows grow at essentially identical asymptotic rates.
- Intermediate mixing regimes (sublinear and superlinear) occur when nonlinearity and heterogeneity compete for the dominance of the mixing dynamics.

We venture a pictorial representation of these results in terms of a "phase-diagram" in the M vs. CV plane. See figure 7. Our results suggest that for a given value of β there is a critical value for the viscosity ratio M (dubbed M_{critical} in the figure). At nearby values, the two-phase flow system behaves according to the several mixing regimes discussed above. The location of the critical value M_{critical} seems to depend on β, being smaller for larger values of β (cf. tables 3 and 4).

7. Concluding remarks

In the study reported here, we investigated the dynamics governing fluid mixing in two-phase, immiscible flows in porous media. Our main results are in the stochastic analysis relating averaged flow to the statistically-described heterogeneities in the geology. Specifically, we assessed the relative importance of nonlinear and stochastic effects in determining large-scale flow regimes. We conducted a parameter study varying the

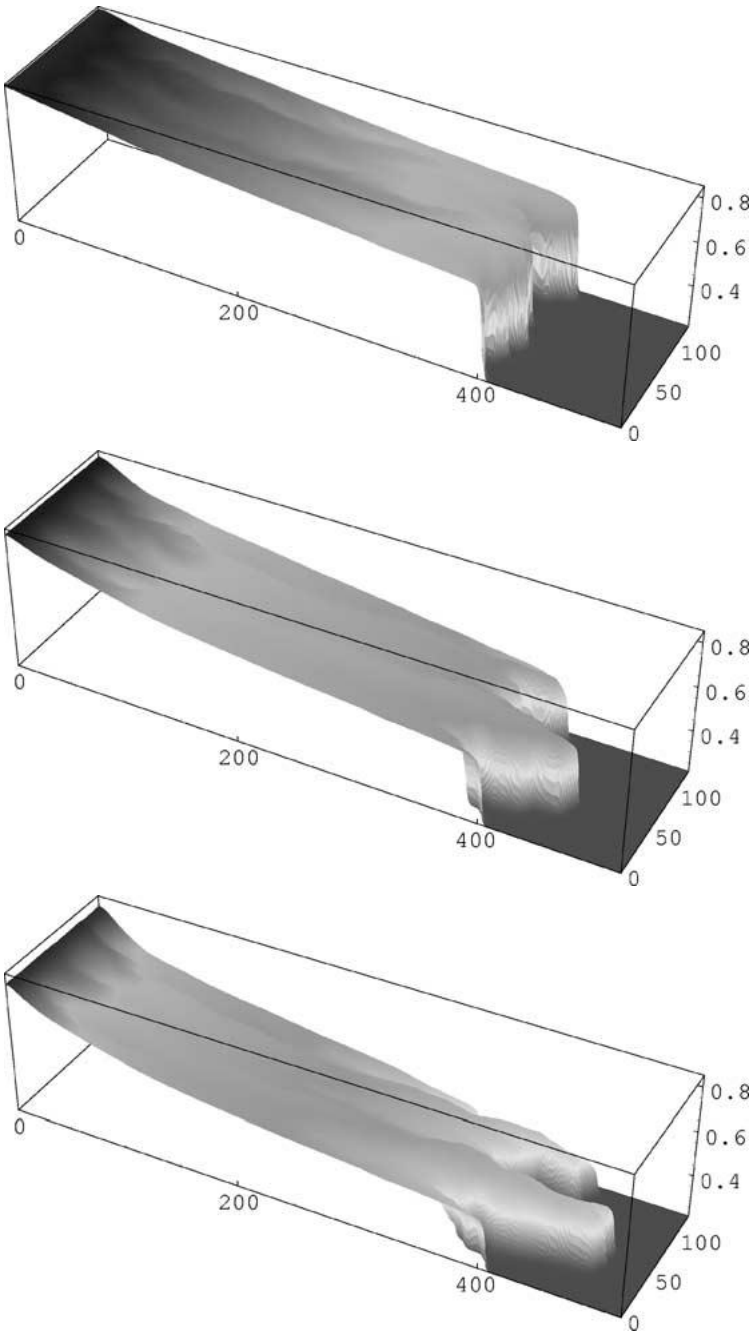

Figure 6. Saturation surface plots displayed as a function of the viscosity ratio M for flow in a $\beta = -0.5$ permeability field with coefficient of variation $CV_k = 0.99$. The values of M, from top to bottom, are $M = 1$, 2.657, 5, and the corresponding mixing regimes are L^- (sublinear), L (linear), and NU (nonlinear unstable); cf. third column of table 4.

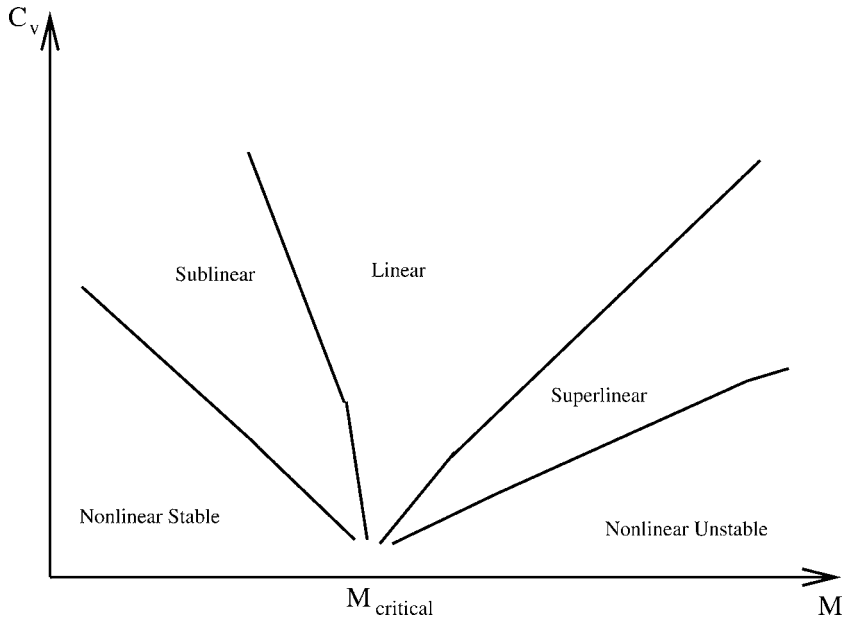

Figure 7. "Phase-diagram": A pictorial representation of the distinct mixing regimes that result from the interplay between nonlinearity and heterogeneity: Nonlinearity controlled regimes NS (nonlinear stable) and NU (nonlinear unstable); heterogeneity controlled regime L (linear); intermediate regimes L^- (sublinear) and L^+ (superlinear).

strength of the nonlinearity relative to the strength of the heterogeneity, and the multiscale nature of the heterogeneity (Hurst exponent). A significant parameter which was not varied in the present study is the degree of layering (anisotropy) in the geology.

Our numerical experiments suggest that the interplay between the nonlinear and stochastic effects depends on their relative strengths. Thus different flow regimes, characterized by the asymptotic scaling behavior of the mixing region, occur as the heterogeneity weakens.

We conclude with a brief discussion relating some of the flow regimes that we have described to the renormalization regimes identified in [17].

Our heterogeneity-dominated regimes pertain to the parabolic renormalization regimes of [17], which are modeled by a parabolic modification of the fluid transport equation (2), viz.,

$$\frac{\partial s}{\partial t} + \mathbf{u} \cdot \nabla f(s) = \nu_{\text{ren}} \Delta s.$$

The renormalized diffusivity ν_{ren}, or macrodiffusivity, is finite if the heterogeneity correlation function decays sufficiently rapidly at large distances (Hurst exponent $\beta < -1$). This is the classical case of Fickian diffusion. Otherwise, i.e., in the case of long range correlations in the heterogeneity field ($-1 < \beta < 0$), the diffusion is anomalous, meaning that ν_{ren} is unbounded and grows with travel distance.

One of our nonlinearity-dominated regimes, the unstable one, relates to the hyperbolic renormalization regime of [17], viz.,

$$\frac{\partial s}{\partial t} + \mathbf{u} \cdot \nabla f_{\text{ren}}(s) = 0,$$

with modest deviation between the renormalized flux f_{ren} and the upper concave envelope (Oleĭnik construction) of the primitive flux function f.

Acknowledgements

This work was supported in part by: the National Science Foundation (NSF) under Grant INT-0104529; FAPERJ under an APQ1 grant and ANP/CNPq under the "Plano Nacional de Ciência e Tecnologia do Setor Petróleo e Gás Natural (CTPETRO)". We are grateful to two anonymous reviewers for their helpful comments on this paper and suggestions. F.F. thanks the Instituto Politécnico da Universidade do Estado do Rio de Janeiro (IPRJ-UERJ) for their hospitality during a stay when this paper was written.

References

[1] L. An, J. Glimm, D.H. Sharp and Q. Zhang, Scale up of flow in porous media, in: *Mathematical Modelling of Flow through Porous Media*, eds. A.P. Bourgeat, C. Carasso, S. Luckhaus and A. Mikelić (World Scientific, New Jersey, 1995) pp. 26–44.

[2] J.W. Barker and S. Thibeau, A critical review of the use of pseudorelative permeabilities for upscaling, SPE Reservoir Engrg. (May 1997) 138–143.

[3] A.J. Chorin, The instability of fronts in a porous medium, Comm. Math. Phys. 91 (1983) 103–116.

[4] R.L. Chouke, P. van Meurs and C. van der Poel, The instability of slow, immiscible, viscous liquid-liquid displacements in permeable media, Trans. AIME 216 (1959) 188–194.

[5] M.A. Christie, Upscaling for reservoir simulations. JPT J. Petrol. Technol. 48 (1996) 1004–1010.

[6] V. Cvetkovic and G. Dagan, Reactive transport and immiscible flow in geological media. II. Applications, Proc. Roy. Soc. London A 452 (1996) 303–328.

[7] G. Dagan, Dispersion of a passive solute in non-ergodic transport by steady velocity fields in heterogeneous formations, J. Fluid Mech. 233 (1991) 1281–1290.

[8] G. Dagan, The significance of heterogeneity of evolving scales to transport in porous formations, Water Resour. Res. 30 (1994) 3327–3336.

[9] G. Dagan and V. Cvetkovic, Reactive transport and immiscible flow in geological media. I. General theory, Proc. Roy. Soc. London A 452 (1996) 285–301.

[10] J. Douglas, Jr., F. Furtado and F. Pereira, On the numerical simulation of waterflooding of heterogeneous petroleum reservoirs, Comput. Geosci. 1(2) (1997) 155–190.

[11] L.J. Durlofsky, Use of higher moments for the description of upscaled, process independent relative permeabilities, SPE 37987 (1997).

[12] Y. Efendiev, L.J. Durlofsky and S.H. Lee, Modeling of subgrid effects in coarse-scale simulations of transport in heterogeneous porous media, Water Resour. Res. 36 (2000) 2031–2041.

[13] F.W. Elliot, Jr. and A. Majda, A wavelet Monte Carlo method for turbulent diffusion with many spatial sales, J. Comput. Phys. 113 (1994) 82–111.

[14] F. Furtado, J. Glimm, B. Lindquist and F. Pereira, Multi-length scale calculations of mixing length growth in tracer floods, in: *Proc. of the Emerging Technologies Conference*, ed. F. Kovarik, Institute for Improved Oil Recovery, University of Houston, Houston, TX, 1990, pp. 251–259.

[15] F. Furtado and F. Pereira, Scaling analysis for two-phase, immiscible flow in heterogeneous media, Comput. Appl. Math. 17 (1998) 233–262.
[16] F. Furtado, F. Pereira and J. Zhu (2002) in preparation.
[17] J. Glimm, H. Kim, D. Sharp and T. Wallstrom, A stochastic analysis of the scale up problem for flow in porous media, Comput. Appl. Math. 17 (1998) 67–79.
[18] J. Glimm, B. Lindquist, F. Pereira and Q. Zhang, A theory of macrodispersion for the scale up problem, Transport Porous Media 13 (1993) 97–122.
[19] J. Glimm, D. Marchesin and O. McBryan, Statistical fluid dynamics: unstable fingers, Comm. Math. Phys. 74 (1980) 1–13.
[20] J. Glimm, D. Marchesin and O. McBryan, A numerical method for two phase flow with an unstable interface, J. Comput. Phys. 39 (1981) 179–200.
[21] J. Glimm and D.H. Sharp, Stochastic partial differential equations: selected applications in continuum physics, in: *Stochastic Partial Differential Equations: Six Perspectives*, eds. R.A. Carmona and B.L. Rozovskii, Mathematical Surveys and Monographs (Amer. Math. Soc., Providence, RI, 1997).
[22] G.M. Homsy, Viscous fingering in porous media, Ann. Rev. Fluid Mech. 19 (1987) 271–311.
[23] K.D. Jarman, Jr., Stochastic immiscible flow with moment equations, Ph.D. thesis, University of Colorado, Boulder (2000).
[24] K.D. Jarman and T.F. Russell, Analysis of 1-D moment equations for immiscible flow, Contemp. Math., to appear.
[25] M.J. King, W.B. Lindquist and L. Reyna, Stability of two-dimensional immiscible flow to viscous fingering, Courant Math. and Comp., Lab. Report DOE/ER/03077-244 (March 1985).
[26] P. Langlo and M. Espedal, Macrodispersion for two-phase, immiscible flow in porous media, Adv. Water Resour. 17 (1994) 297–316.
[27] R. Lenormand, Determining flow equations from stochastic properties of a permeability field: The MHD model, SPE J. (June 1996) 179–190.
[28] H. Nessyahu and E. Tadmor, Non-oscillatory central differencing for hyperbolic conservation laws, J. Comput. Phys. 87(2) (1990) 408–463.
[29] H. Rajaram and L.W. Gelhar, Plume scale-dependent dispersion in heterogeneous aquifers, 2. Eulerian analysis and three-dimensional aquifers, Water Resour. Res. 29 (1993) 3261–3271.
[30] P. Saffman and G. Taylor, The penetration of a fluid into a porous medium or Hele–Shaw cell containing a more viscous liquid, Proc. Roy. Soc. London A 245 (1958) 312–322.
[31] J. Smoller, *Shock Waves and Reaction–Diffusion Equations* (Springer, New York, 1983).
[32] J.R. Waggoner, J.L. Castillo and L.W. Lake, Simulation of EOR processes in stochastically generated permeable media, SPE 21237, SPE Formation Evaluation (June 1992) 173–180.
[33] T. Wallstrom, S. Hou, M.A. Christie, L.J. Durlofsky and D.H. Sharp, Accurate scale up of two-phase flow using renormalization and nonuniform coarsening, Comput. Geosci. 3 (1999) 69–87.
[34] T. Wallstrom, S. Hou, M.A. Christie, L.J. Durlofsky and D.H. Sharp, Application of a new two-phase upscaling technique to realistic reservoir cross sections, in: *Proc. of the SPE 15th Symposium on Reservoir Simulation*, SPE 51939, 1999, pp. 451–462.
[35] T. Wallstrom, S. Hou, M.A. Christie, L.J. Durlofsky, D.H. Sharp and Q. Zhou, Effective medium boundary conditions for upscaling relative permeabilities, Transport Porous Media (2000) accepted for publication.
[36] D. Zhang, L. Li and H.A. Tchelepi, Stochastic formulation for uncertainty analysis of two-phase flow in heterogeneous reservoirs, SPE J. 5 (2000) 60–70.
[37] Q. Zhang, A multi-length scale theory of the anomalous mixing length growth for tracer flow in heterogeneous porous media, J. Statist. Phys. 66 (1991) 485–501.
[38] J. Zhu, A numerical study of stochastic dispersion for two-phase immiscible flow in porous media, M.Sc. thesis, University of Wyoming (2001).